© 2023. Published by The Company of Biologists Ltd | Journal of Experimental Biology (2023) 226, jeb245199. doi:10.1242/jeb.245199

RESEARCH ARTICLE

Muscle force–length dynamics during walking over obstacles indicates delayed recovery and a shift towards more 'strut-like' function in birds with proprioceptive deficit

M. Janneke Schwaner[1,*], Joanne C. Gordon[2], Andrew A. Biewener[3] and Monica A. Daley[1,4]

ABSTRACT

Recent studies of *in vivo* muscle function in guinea fowl revealed that distal leg muscles rapidly modulate force and work to stabilize running in uneven terrain. Previous studies focused on running only, and it remains unclear how muscular mechanisms for stability differ between walking and running. Here, we investigated *in vivo* function of the lateral gastrocnemius (LG) during walking over obstacles. We compared muscle function in birds with intact (iLG) versus self-reinnervated LG (rLG). Self-reinnervation results in proprioceptive feedback deficit due to loss of monosynaptic stretch reflex. We tested the hypothesis that proprioceptive deficit results in decreased modulation of EMG activity in response to obstacle contact, and a delayed obstacle recovery compared with that for iLG. We found that total myoelectric intensity (E_{tot}) of iLG increased by 68% in obstacle strides (S 0) compared with level terrain, suggesting a substantial reflex-mediated response. In contrast, E_{tot} of rLG increased by 31% in S 0 strides compared with level walking, but also increased by 43% in the first post-obstacle (S +1) stride. In iLG, muscle force and work differed significantly from level walking only in the S 0 stride, indicating a single-stride recovery. In rLG, force increased in S 0, S +1 and S +2 compared with level walking, indicating three-stride obstacle recovery. Interestingly, rLG showed little variation in work output and shortening velocity in obstacle terrain, indicating a shift towards near-isometric strut-like function. Reinnervated birds also adopted a more crouched posture across level and obstacle terrains compared with intact birds. These findings suggest gait-specific control mechanisms in walking and running.

KEY WORDS: Proprioception, *In vivo* muscle dynamics, Sensorimotor control, Reinnervation, Locomotion, Obstacle navigation

INTRODUCTION

Bipedal locomotor dynamics

Striding bipeds walk at slow speeds and run at higher speeds, and these gaits exhibit differing body center of mass (CoM) mechanics. During walking, the leg acts as a relatively stiff compressive strut during stance and the body vaults over the leg like an inverted pendulum, with the body reaching its highest point at midstance, whereas during running, the leg is compliant and compresses so the body reaches its lowest point at midstance (Cavagna and Kaneko, 1977; McMahon and Cheng, 1990; Farley and Farris, 1998). Despite these differences in CoM dynamics, walking and running can both be modeled as a spring-loaded inverted pendulum (SLIP), consisting of a body mass on a compliant spring leg (Geyer et al., 2006). The SLIP model has two basic modes of motion, (1) leg length compression and extension, regulated by effective leg stiffness, and (2) leg angular cycling, actuated by hip flexion and extension (McGeer, 1990a,b; McMahon and Cheng, 1990). Achieving robustly stable bipedal locomotion requires precise coordination of these two basic modes of leg motion, with appropriate modulation to enable controlled variation in speed (Farley et al., 1993).

Control mechanisms for bipedal legged locomotion

Locomotor control involves integration of sensory information in a hierarchically organized system that includes spinal reflexes, rhythmic spinal networks and input from the brain transmitted via descending pathways (Dickinson et al., 2000; Pearson, 2000; Frigon and Rossignol, 2006; Nishikawa et al., 2007; Prochazka and Ellaway, 2012). Within this hierarchy, we use 'feedforward' control to refer to the contributions by motor commands arising from the descending pathways and rhythmic spinal networks, generated based on the anticipated demands of the task (Pearson, 2000; Frigon and Rossignol, 2006). 'Feedback' control refers to the modulation of motor output by sensorimotor reflexes in the spinal cord, in response to estimated errors in movement during the interaction between the body and the environment. Integration of feedforward and feedback control is essential for versatile and stable movement. Feedforward control provides appropriate muscle co-activation and coordination in anticipation of mechanical demands, and feedback control corrects errors due to unexpected perturbations and changes in task demands. However, time delays inherent to animal nervous systems limit the speed of sensorimotor feedback (More and Donelan, 2018). These delays can become limiting with increasing speed, because response times become longer relative to movement duration (More and Donelan, 2018). For example, the average stance period in running guinea fowl is ∼118 ms, and the short latency reflex delay is 40 ms (Daley et al., 2009), which is 33% of the stance phase in running. In comparison, during walking (∼0.7–1.0 m s^{-1}; Schwaner et al., 2022; Gatesy, 1999), the short latency reflex response is only 11–13% of the stance duration. As a result, control mechanisms shift with increasing speed, with lower reflex feedback gains in running compared with walking (Capaday and Stein, 1987; Stein and Capaday, 1988; Edamura et al., 1991; Gordon et al., 2015; Daley, 2018). Consequently, at high speeds,

[1]Department of Ecology and Evolutionary Biology, University of California, Irvine, Irvine, CA 92697, USA. [2]Comparative Biomedical Sciences, Royal Veterinary College, University of London, London NW1 0TU, UK. [3]Organismic and Evolutionary Biology, Harvard University, Cambridge, MA 02138, USA. [4]Center for Integrative Movement Sciences, University of California, Irvine, Irvine, CA 92617, USA.

*Author for correspondence (mjschwan@uci.edu)

M.J.S., 0000-0002-1666-3111; A.A.B., 0000-0003-3303-8737; M.A.D., 0000-0001-8584-2052

Received 17 October 2022; Accepted 16 May 2023

animals are expected to rely more on feedforward motor output and intrinsic mechanical control mechanisms to maintain stability, but at slow speeds, corrective reflex feedback plays a larger role in the response to perturbations.

In vivo measures of muscle activity during perturbation responses can provide insight into how feedforward, feedback and intrinsic mechanics are integrated for effective movement control (Mortiz and Farley, 2004; Daley et al., 2009; Daley and Biewener, 2011). Because of sensorimotor delays, the initial response to a perturbation depends on the combination of feedforward activation and intrinsic mechanical responses. Contributions of reflex feedback to motor activity can be inferred based on the timing of electromyography (EMG) changes relative to a perturbation. For example, humans use reflex-mediated responses to adjust leg stiffness in response to a sudden, unexpected increase in substrate stiffness, with a delay of ∼100 ms for the response. With foreknowledge of the upcoming change, participants use feedforward increases in activity starting before the perturbation to achieve the same effective leg stiffness (Mortiz and Farley, 2004). These findings demonstrate flexibility and redundancy in sensorimotor control systems that allow the same locomotor task to be accomplished by multiple possible mechanisms. Nevertheless, it remains unclear how, and on what time scales, feedforward, feedback and intrinsic mechanical mechanisms are tuned to provide coordinated and stable locomotion.

Guinea fowl as a model for bipedal locomotion

Guinea fowl have become a well-established animal model for investigating neuromechanical control of bipedal locomotion. Direct, *in vivo* measurements of muscle force, length and activation dynamics can reveal how intrinsic muscle dynamics contribute to perturbation responses and stability mechanisms. Additionally, these studies provide insight into the integration of neuromechanical factors across structural scales from muscle fascicles to muscle–tendon units, to joint, limb and body dynamics. Previous studies of neuromechanics in guinea fowl have focused on perturbation responses in fast locomotion, to understand the contributions of intrinsic mechanical responses to stability (Daley and Biewener, 2006; Daley et al., 2009; Birn-Jeffery et al., 2014; Gordon et al., 2020). The initial, rapid response to a perturbation arises directly from the intrinsic mechanics of the musculoskeletal system, before a neural response is possible (Brown and Loeb, 2000; Jindrich and Full, 2002).

A major hindlimb extensor muscle in guinea fowl, the lateral gastrocnemius (LG) develops force during stance to support body weight and produces positive work to contribute to propulsion through leg length actuation (Daley and Biewener, 2003; Daley et al., 2009; Daley and Biewener, 2011; Gordon et al., 2020). The LG plays an important role in the intrinsic mechanical response to perturbations because it is activated in late swing in anticipation of stance and begins to develop force just before foot contact. EMG activity of guinea fowl LG in steady locomotion has both feedforward and feedback components, with an initial burst of activity that begins before stance, and a second burst of activity that occurs after foot contact and varies in magnitude and duration based on feedback (Gordon et al., 2020). This pattern also has been observed in cats (Wilmink and Nichols, 2003; Donelan and Pearson, 2004) and humans (Dietz et al., 1979). When guinea fowl run over uneven terrain, the timing of foot contact and leg loading is altered relative to the timing of feedforward activation. Variation in the timing of load relative to activation results in altered muscle force–length dynamics and limb posture. These altered intrinsic mechanics help to rapidly stabilize the body CoM in response to the terrain perturbations (Daley and Biewener, 2006; Daley et al., 2007, 2009; Daley and Biewener, 2011). For example, when guinea fowl encounter an unexpected terrain drop, postural changes result in shorter muscle length of the LG during stance, and a ∼70% reduction in muscle force despite a similar activation level (Daley et al., 2009). Lower muscle force during stance results in energy absorption by the LG, thereby providing stability without a reflex response. Studies of running over uneven terrain in guinea fowl have therefore highlighted the importance of muscle force–length dynamics and postural changes for control of stable locomotion at high speeds.

LG function and control mechanisms in walking and running

Considering that most studies of guinea fowl neuromuscular function have focused on fast speeds, the differences in control mechanisms between walking and running remain unclear. In a study of muscle activity during walking and running over obstacles, Gordon and colleagues (2015) found that guinea fowl exhibit larger feedforward increases in muscle activity during running but show larger stride-to-stride reflex-mediated modulation of activity while walking. These differences in control mechanisms between the two gaits also result in higher variation in stride duration in walking compared with running. Additionally, visual cues exert a larger influence on muscle activity at slower speeds compared with higher speeds, likely as a result of the longer processing times involved in visuomotor regulation of hindlimb spinal networks. Overall, previous studies in humans and guinea fowl suggest that walking relies more heavily on short and long latency feedback compared with running, which relies more on feedforward and intrinsic mechanical mechanisms (Capaday and Stein, 1987; Stein and Capaday, 1988; Edamura et al., 1991; Gordon et al., 2015; Daley, 2018). However, none of these previous studies, including those on guinea fowl, have measured muscle force–length dynamics during normal versus perturbed walking, and it remains unclear how reflex responses are integrated with intrinsic muscle dynamics and postural mechanisms of control.

Reinnervation as a manipulation of control mechanisms

Surgical self-reinnervation can be a useful manipulation to investigate neuromechanical control mechanisms in locomotion. Self-reinnervation results in short-term muscle paralysis followed by motor recovery, with long-term loss of proprioception in the reinnervated muscle (Abelew et al., 2000; Maas et al., 2007; Gordon et al., 2020). Once fully recovered, guinea fowl with self-reinnervated LG achieve similar overall gait dynamics and stabilizing responses while running at high speeds over obstacles (Gordon et al., 2020). Likewise, quadrupedal animals such as cats and rats also recover similar gait dynamics in response to reinnervation (Chang et al., 2009, 2018; Bauman and Chang, 2013). Running birds compensate for proprioceptive deficit in LG through a feedforward increase in activation and a more flexed ankle in stance, which together likely help to maintain high ankle stiffness (Gordon et al., 2020). Birds with reinnervated LG lack regulation of the duration of activity in late stance, which is present in the intact birds. These findings support the hypothesis that reflex feedback contributes to regulating the duration of muscle activity in stance. However, these findings were based on running speeds only, and it is not clear whether guinea fowl use similar mechanisms to compensate for proprioceptive deficit while walking.

Here, we investigated how guinea fowl integrate muscle dynamics and sensorimotor control to achieve stable walking on

an obstacle treadmill. We hoped to gain insight into the role of reflexes and the mechanisms that enable recovery of function in their absence, by comparing *in vivo* neuromuscular dynamics and kinematics of walking over obstacle terrain in intact versus reinnervated birds. Based on the findings summarized above, we hypothesized that LG proprioceptive deficit will elicit decreased modulation of EMG activity in response to obstacles, and a slower obstacle recovery compared with that in intact birds. Decreased modulation of EMG activity is likely to lead to several changes in the neuromechanical control of walking because of the complex interaction between motor control, muscle dynamics and biomechanics of gait.

MATERIALS AND METHODS

Animals

All data presented here were collected as part of a larger study on the same cohorts of individuals; however, only data at running speeds were previously analyzed and published (Daley and Biewener, 2011; Gordon et al., 2020). Running data from the intact cohort data (n=6 guinea fowl, 1.77±0.63 kg body mass, mean±s.d.) were initially published in Daley and Biewener (2011) and running data from the reinnervated cohort (n=6 guinea fowl, body mass of 1.81 ±0.28 kg) were published by Gordon et al. (2020). Complete details on the experimental methods for each cohort can be found in these two publications. Here, we briefly describe the methods and present the previously unpublished walking data. All experiments were undertaken at the Concord Field Station of Harvard University, in Boston (MA, USA), and all procedures were licensed and approved by the Harvard Institutional Animal Care and Use Committee (AEP #20-09) in accordance with the guidelines of the National Institutes of Health and the regulations of the United States Department of Agriculture.

Self-reinnervation procedures

Six guinea fowl *Numida meleagris* (Linnaeus 1758) underwent a surgical procedure at 7–12 weeks old under isoflurane anesthesia (1.5–3%, mask/intubation delivery) to bilaterally transect and immediately repair the peripheral nerve branches of the LG muscles (Gordon et al., 2020). During the reinnervation surgery, lateral incisions were made posterior–distal to the knee joint. With the use of blunt dissection techniques, the nerve branch was exposed. Before transecting the nerve, 6-0 braided silk suture (Silk, Ethicon, Somerville, NJ, USA) was passed through the nerve. This suture was used to oppose the nerve endings after transection. Fibrin glue was used as a means of second repair scaffold over the nerve endings. Fascia and skin were closed with 3-0 braided absorbable poly-glactin (Vicryl, Ethicon, Somerville, NJ, USA). Animals were allowed to fully recover motor function before transducer surgeries took place (see below), 13–16 weeks following the reinnervation surgical procedure. After recovery, proprioceptive deficit was confirmed by the absence of the muscle's short-latency tendon-tap response. For further details on recovery trajectories and monitoring, see Gordon et al. (2020).

In vivo transducer implantation

Transducer implantation surgeries were carried out under isoflurane anesthesia (1.5–3%, mask/intubation delivery), following procedures similar to Daley and Biewener (2003, 2011). Feathers were removed from the leg to be instrumented, and the surgical field was cleaned with antiseptic solution (Prepodyne, West Argo, Kansas City, MO, USA). Transducer leads were tunneled under the skin, starting from a ∼20 mm incision over the synsacrum to a 50 mm incision over the lateral shank. Sonomicrometry crystals (2.0 mm; Sonometrics Inc., London, ON, Canada) were implanted along muscle fascicles of the LG. Transducer signals were checked using an oscilloscope before securing and closing muscle fascia with 4-0 silk suture (Silk, Ethicon, Somerville, NJ, USA). Bipolar EMG electrodes (AS 632 Teflon-coated stainless steel wire: Cooner Wire Co., Chatsworth, CA, USA) were implanted in the middle third of the muscle belly. A custom-designed 'E'-type stainless steel tendon buckle force transducer was secured around the common gastrocnemius tendon. All implanted transducers were connected through a micro-connector plug (15-way Micro-D, Farnell Ltd, Leeds, UK), which was secured by suture to the bird's dorsal synsacrum.

Data collection and analysis

Animals were trained to walk on a treadmill (Woodway, Waukesha, WI, USA) with and without obstacles (Gordon et al., 2020). Animals were encouraged to steadily locomote at a walking speed of 0.8 m s^{-1}. We recorded high-speed video (250 Hz, Photron, San Diego, CA, USA) for kinematics analysis and stride timings.

We assigned stride categories in relation to the timing of obstacle encounters (after Daley and Biewener, 2011, and Gordon et al., 2020). These categories were based on the stride sequence of the instrumented leg and were as follows: S −1 (stride prior to obstacle contact), S 0 (stride with obstacle contact), S +1 (first stride following obstacle contact), and S +2 (second stride following obstacle contact). Level terrain strides were all assigned to the level category (Level). Based on their surgical condition, birds are assigned a cohort, intact (I) and reinnervated (R).

We measured LG muscle shortening, EMG activation, and force–length dynamics and work output (similar to Daley and Biewener, 2011; Gordon et al., 2020). We obtained myoelectric intensities from raw EMG signals in time and frequency using wavelet decomposition, with wavelets optimized for muscle (after Von Tscharner, 2000; Wakeling et al., 2002; Daley et al., 2009; Gordon et al., 2015). The total intensity at each time point was calculated based on the sum across wavelet frequencies. We integrated EMG intensity over the stride period to calculate total myoelectric intensity per stride (E_{tot}). We also calculated the mean frequency of muscle activation (E_{freq}). To evaluate timing of EMG relative to muscle length trajectory, we calculated the phase difference between the EMG intensity trajectory and the muscle length trajectory, normalized to a fraction of the stride cycle (E_{phase}). Specifically, we took the time difference between 50% E_{tot} and peak muscle length and divided that value by the stride duration. Fractional fascicle length (L) data were obtained from sonomicrometry data using mean length in level terrain as a reference length (L_0). In the present study, L_0 is not directly related to sarcomere length or the muscle's optimal length for isometric force–length curves, because these were not measured. Fascicle velocity (V) in lengths per second (L s^{-1}) was calculated based on the differentiation of fractional fascicle length. Shortening length and velocity are negative. Fascicle velocity in m s^{-1} was multiplied by tendon force (in N) to obtain muscle power (in W), which was integrated in time to obtain work per stride (in J; with shortening work being positive), and normalized by muscle mass (Gordon et al., 2020) to calculate mass-specific muscle work (in J kg^{-1}).

In evaluating an individual's obstacle perturbation responses, the relevant metric is the deviation from that individual's mean value for steady level running at the same speed. The absolute magnitude of these deviations can vary between individuals as a result of differences in steady-state values, differences in body size and

Journal of Experimental Biology (2023) 226, jeb245199. doi:10.1242/jeb.245199

varying electrode placement and geometry. Consequently, to effectively compare responses across individuals and between the intact and reinnervated cohort, we divided measures of muscle fractional length, muscle force and EMG activity by their respective mean value during level walking (L_c, F_c and E_c, respectively), resulting in a fractional change from the steady condition. To normalize trajectories of muscle length, force and EMG activity, we divided each trajectory by the mean muscle length (L_{mean}), maximum force (F_{max}) and peak EMG activity (E_{max}), respectively, for steady level terrain. All data processing was completed using in-house code in MATLAB (Mathworks, Inc., Natick, MA, USA).

We obtained leg joint kinematics and CoM dynamics from video recordings (collected at 250 Hz; Photron, San Diego, CA, USA) that were digitized using DeepLabCut (version 2.2) (Mathis et al., 2018; Nath et al., 2019). We digitized markers on the toe tip, tarsometatarsal, foot, ankle and knee joints, and the location of the transducer connector. We used six body markers along the chest and the back to estimate the location of the CoM. We used ∼40 frames from 5 videos, across the different data collection days for each animal to train DeepLabCut. We used a ResNet-50-based neural network with default parameters for a minimum of 750,000 training iterations. Each trained network was used to analyze all videos from the same animal. We filtered raw marker location data using a Butterworth filter with a cut-off frequency of 30 Hz, before further processing in MATLAB.

We calculated leg length and body CoM height to quantify the gait dynamics. We calculated leg length (LL) as the distance between the CoM and foot, scaled as a percentage of the sum of all leg segment lengths (Rubenson and Marsh, 2003; Schwaner et al., 2022). We also calculated leg angle (LA), represented by the angle between a virtual leg (e.g. a line vector between the foot and CoM) and the ground. We calculated net and maximum joint angles for the hip, knee, ankle and tarsometatarsal–phalangeal (TMP) joint.

Statistical analysis

We used a linear mixed-effects ANOVA with stride category and surgical condition (intact/reinnervated) as fixed factors, and individual as a random factor. We compared multiple models: Model 1 included only the intercept and individual as a random effect [Y ∼ 1 + (1|ind)], used as a reference model and null hypothesis, which was then compared with three alternative models: Model 2 with stride category (StrideCat) as a categorical fixed effect [Y ∼ 1 + StrideCat+(1|ind)], Model 3 with surgical treatment (Treatment) as a categorical fixed effect [Y ∼ 1 + Treatment+(1|ind)], Model 4 with both StrideCat and Treatment as independent fixed effects [Y ∼ 1 + StrideCat+Treatment+(1|ind)], and Model 5 with an interaction term between fixed effects [Y ∼ 1 + StrideCat*Treatment+(1|ind)]. We compared candidate models based on AIC, total adjusted R^2 and log-likelihood ratio tests, which supported selection of Model 5 across all variables tested. Muscle variables tested were total EMG intensity over the stride (E_{tot}), EMG activity duration (E_{dur}), median EMG frequency (E_{freq}), phase relationship between length and EMG as a fraction of stride cycle (E_{phase}), net work output (W_{net}), peak force (F_{pk}), force duration (F_{dur}), velocity at peak force (V_{pk}), mean velocity during EMG activation ($V_{mean,act}$), length at peak force (L_{pk}) and length at 50% force impulse ($L_{imp,T50}$) as a measure of length during early stance. Kinematic variables analyzed included stance period, stride period, CoM height at foot contact (T_{on}), leg length (LL) and leg angle (LA) at foot contact, net change in leg length and angle, the joint angles at T_{on}, net change in joint angles during stance, and maximum angle change during stance. For each variable analyzed, we first calculated the ANOVA test statistics, and if the fixed effects were found to be statistically significant after false discovery rate correction, we then calculated 95% confidence intervals (CIs) for the treatment effect and the pairwise difference from obstacle stride categories and level terrain. Pairwise differences are based on marginal means after accounting for the random effects.

RESULTS

LG function in level locomotion: intact and reinnervated guinea fowl

During level walking, iLG was activated and began to shorten in late swing, before foot contact, resulting in a slow rise in muscle force in late swing, followed by a sharp rise in force at the time of foot contact, reaching a peak force before midstance (Fig. 1). The iLG muscle contracted near isometrically during the steep force rise and shortened at a low rate from mid to late stance, resulting in net positive work during walking. In birds with rLG, the general pattern of rLG force–length dynamics over the course of the stride cycle was similar to that of iLG. The traces in Fig. 1 are from representative individuals only and should not be interpreted as indicating statistically significant differences between the surgical treatment groups, which are discussed in detail below. The shape of the EMG trajectory tended to be idiosyncratic and unique to each individual. Summary statistics for muscle morphology and mechanical output for steady-state level strides of the iLG and rLG are presented in Table 1.

LG force–length trajectories during obstacle encounters

When walking guinea fowl with intact LG encountered an obstacle (S 0), the foot contacted the substrate earlier, and this was associated with an earlier rise in muscle force. The iLG muscle length remained longer in S 0 and showed no isometric phase in early stance. The iLG shortened at a steady rate throughout force development during the stance phase of obstacle encounters (Fig. 2, blue traces in S 0). Average iLG shortening velocity was higher in perturbed strides compared with level strides, which, along with higher peak force, resulted in higher iLG work output in S 0. Intact birds recovered from the obstacle encounter within one stride, with only the perturbed obstacle stride S 0 differing significantly from level terrain locomotion across most measured variables. Reinnervated birds exhibited similar overall trends when negotiating the obstacle; however, rLG maintained a slower average shortening velocity throughout stance in the obstacle stride compared with the obstacle stride of iLG (Fig. 3, orange traces in S 0).

Shifts in muscle activity patterns during obstacle negotiation: iLG versus rLG

iLG exhibited a 68% increase in muscle activation (E_{tot}) on obstacle encounter strides (S 0) compared with steady-state level at the same speed. No other strides significantly differed from level terrain, indicating a one-stride recovery response (Fig. 4, Table 2). EMG duration (E_{dur}) was slightly but not significantly longer in S 0 compared with level terrain. However, E_{dur} was slightly shorter compared with level terrain in all non-obstacle strides in the obstacle terrain, which likely relates to the slightly shorter average stance and stride period in non-perturbed strides in obstacle terrain compared with level terrain (Tables 2 and 3).

In comparison to iLG, rLG exhibited a smaller fractional increase of 31% E_{tot} in the obstacle stride relative to level terrain (Fig. 4, Table 2). Reinnervated birds showed more pronounced deviations

Journal of Experimental Biology (2023) 226, jeb245199. doi:10.1242/jeb.245199

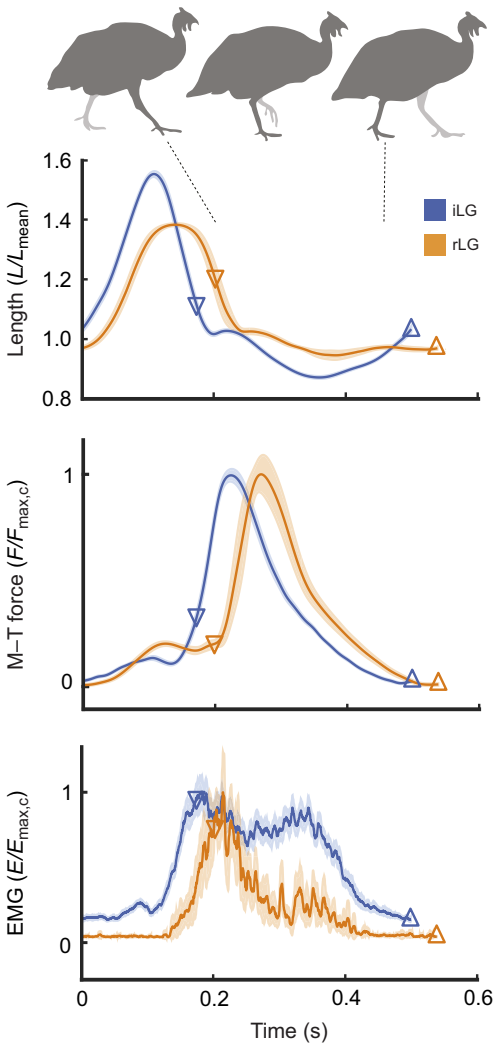

Fig. 1. Average trajectories of *in vivo* lateral gastrocnemius (LG) muscle recordings for representative individuals during level walking. Traces show the mean±95% confidence interval (CI) for muscle length, muscle–tendon (M–T) force and electromyography (EMG) activity, averaged over a complete stride cycle. Muscle length is presented as the fractional length, calculated by dividing the muscle length trajectory (L) by the mean muscle length (L_{mean}) for an individual. M–T force is given as force (F) divided by the maximum force during level walking ($F_{max,c}$). EMG is given as EMG intensity (E) divided by the maximum EMG during level walking ($E_{max,c}$). Data are presented for a representative intact bird (Ind 30) and a reinnervated bird (Ind 2). Triangles indicate the timing of foot on (downward pointing) and foot off (upward pointing). Intact (iLG) and reinnervated LG (rLG) exhibit similar patterns of force–length dynamics over the course of the stride cycle. This figure presents data from representative individuals only and should not be interpreted as indicating statistically significant differences between individuals or surgical treatment cohorts. In particular, EMG trajectories tend to be idiosyncratic and unique per individual.

from level in the post-obstacle recovery strides (S +1 and S +2) (Fig. 4, Table 2). For example, rLG showed an increase of 43% E_{tot} in S +1 in reinnervated birds, whereas iLG showed no significant difference from level in S +1. rLG also showed a trend towards 55 ms longer EMG duration across all stride categories compared with iLG (Fig. 4B, ΔE_{dur}, I–R, gray bar). However, this trend was not statistically significant because of high variance (Table 2). rLG also exhibited a narrower distribution of EMG frequency with a trend towards higher frequency compared with iLG, but this was

Table 1. Summary statistics for muscle morphology and mechanical output for steady level walking for intact and reinnervated lateral gastrocnemius (LG)

Variable	Intact	Reinnervated
W_{net} (J kg^{-1})	2.64±0.38	2.62±0.69
F_{pk} (N)	35.34±10.60	28.74±4.94
Mean force (N)	10.10±3.28	9.51±1.76
Force duration (s)	0.23±0.05	0.24±0.03
Body mass (kg)	1.77±0.58	1.82±0.26
Muscle mass (g)	24.74±6.63	28.09±3.27
Fiber length (mm)	18±1.41	17±0.64
Pennation angle (deg)	24.17±4.67	25.08±4.31

Values are means±s.d. W_{net}, net work output; F_{pk}, peak force.

also non-significant (Fig. 4, Table 2). Lastly, we found that rLG showed a delay in the phase of EMG intensity relative to muscle length (E_{phase}) in obstacle strides (Table 2, S 0). This change in phase was not present in S 0 of intact birds, despite a larger fractional increase in E_{tot}.

Shifts in muscle force–length dynamics and work output during obstacle negotiation: iLG versus rLG

iLG showed a 3.6 J kg^{-1} increase in net work output (W_{net}) in the obstacle strides (S 0) compared with level strides, whereas rLG showed a smaller increase of only 0.7 J kg^{-1} in S 0 compared with level walking (Fig. 5, Table 2). However, rLG showed a 43% increase in peak force (F_{pk}) in S 0 compared with level strides, whereas iLG showed only a 22% increase in F_{pk} in S 0 compared with level walking (Fig. 5, Table 2). rLG showed a significant increase in F_{pk} in S 0, S +1 and S +2 compared with level strides, indicating three-stride obstacle recovery (Fig. 5, Table 2). In contrast, F_{pk} increased only in the obstacle contact strides for intact birds (Fig. 5, Table 2), indicating a one-stride recovery. Intact birds showed a pronounced increase in LG shortening velocity at peak force (V_{pkF}) in S 0, indicated by negative values for V_{pkF} compared with level walking (Fig. 5, S 0), but no such change was present in rLG in S 0. There were no significant differences in V_{pk} among obstacle strides in the reinnervated cohort (Fig. 5, Table 2).

Intact and reinnervated birds exhibited comparable changes in LG fractional length (L/L_c) at peak force (L_{pkF}) in obstacle strides, but rLG exhibited slightly shorter active lengths in unperturbed strides in obstacle terrain (Fig. 5). For iLG, only S 0 exhibited a longer L_{pkF} compared with level strides, whereas rLG exhibited significant differences in L_{pkF} across all obstacle terrain strides compared with level strides (Fig. 5, Table 2).

Timing of obstacle-induced changes in EMG activity in relation to changes in length and force

To evaluate the timing of obstacle-induced shifts in EMG activity relative to perturbations in force and length, we calculated the difference between the average obstacle stride trajectory (S 0) and the average steady level trajectory (Fig. 6). Significant changes in iLG force and EMG were not apparent until obstacle contact. An increase in iLG EMG occurred after an increase in force, suggesting a reflex-mediated response to increased load applied to the active muscle (Fig. 6). rLG also showed an increase in force after obstacle contact and preceding any change in EMG, similar to intact birds However, the change in rLG EMG in response to the obstacle perturbation was less pronounced and more variable, consistent with a proprioceptive deficit. rLG also exhibited larger deviations in length between in the obstacle perturbed trajectory compared with steady state, especially in late stance.

Journal of Experimental Biology (2023) 226, jeb245199. doi:10.1242/jeb.245199

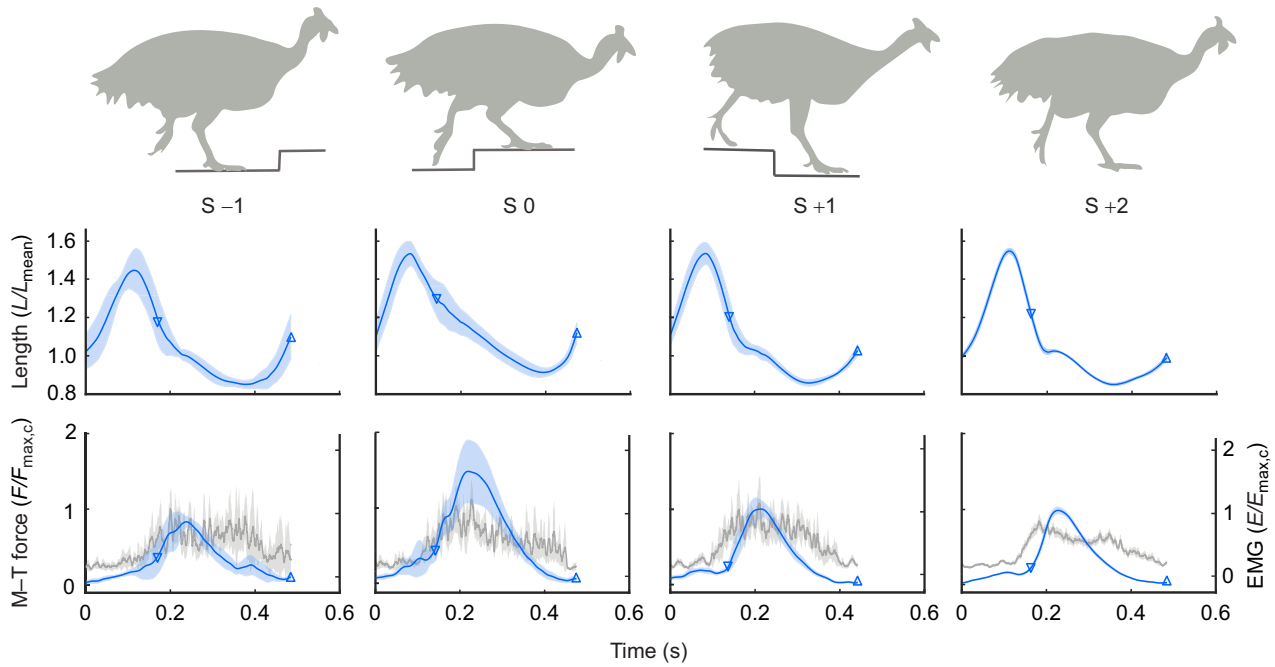

Fig. 2. Average trajectories of *in vivo* LG muscle recordings across stride categories for a representative intact individual (Ind 30) during obstacle terrain walking. Traces show the mean±95% CI for muscle fractional length, force (bottom left *y*-axis, blue) and EMG activity (bottom right *y*-axis, gray), averaged over stride cycles within each stride category (S −1, stride prior to obstacle contact; S 0, stride with obstacle contact; S +1, first stride following obstacle contact; and S +2, second stride following obstacle contact). Downward pointing triangles indicate foot–ground contact (T_{on}), and upward pointing triangles indicate time of foot off (T_{off}). During obstacle contact, intact LG exhibits higher force compared with level walking and relatively greater shortening during the obstacle stride.

Work loop patterns in iLG versus rLG

In level treadmill locomotion, both iLG and rLG developed force and shortened during stance to produce a counterclockwise work loop indicating positive work (Fig. 7). iLG exhibited rapid shortening just before stance, with near-isometric contraction following foot contact until peak force, followed by shortening in

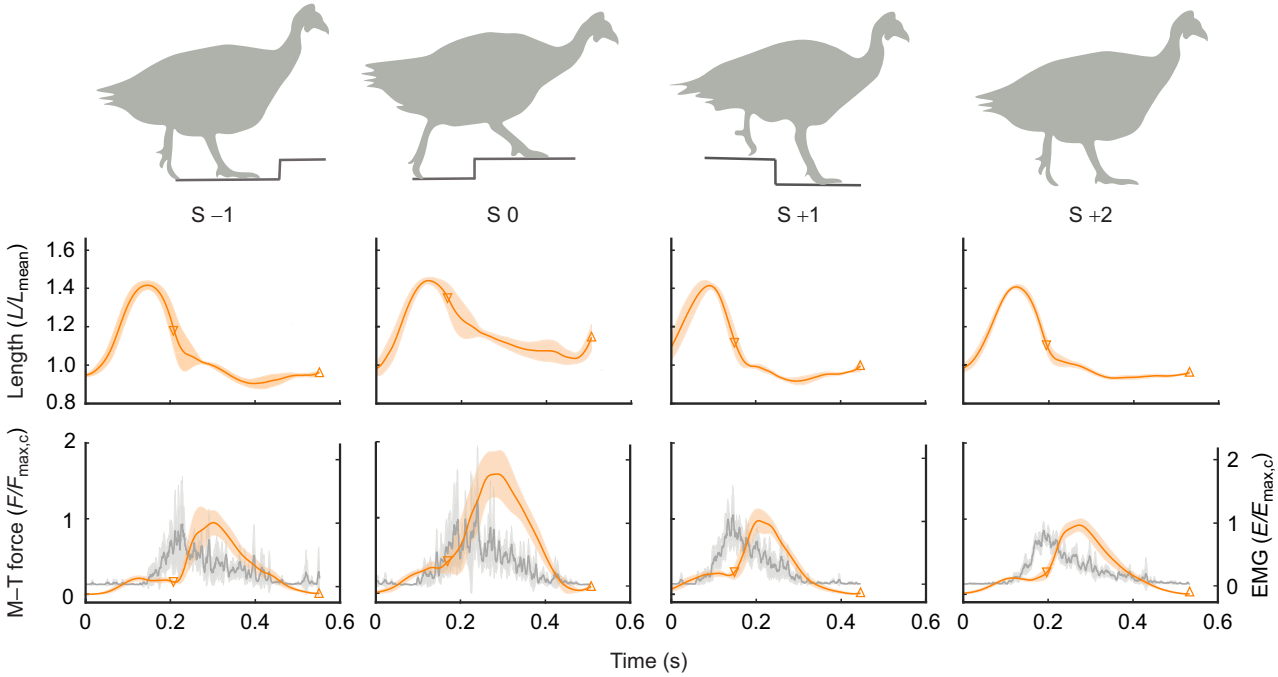

Fig. 3. Average trajectories of *in vivo* LG muscle recordings across stride categories for a representative reinnervated individual (Ind 2) during obstacle terrain walking. Traces show the mean±95% CI for muscle fractional length, force (bottom left *y*-axis, blue) and EMG activity (bottom right *y*-axis, gray), averaged over stride cycles within each stride category (S −1, S 0, S +1 and S +2). Downward pointing triangles indicate foot–ground contact (T_{on}), and upward pointing triangles indicate time of foot off (T_{off}). Upon encountering the obstacle, reinnervated LG exhibits increased force development, but little change in shortening during the obstacle stride compared with level walking.

Journal of Experimental Biology (2023) 226, jeb245199. doi:10.1242/jeb.245199

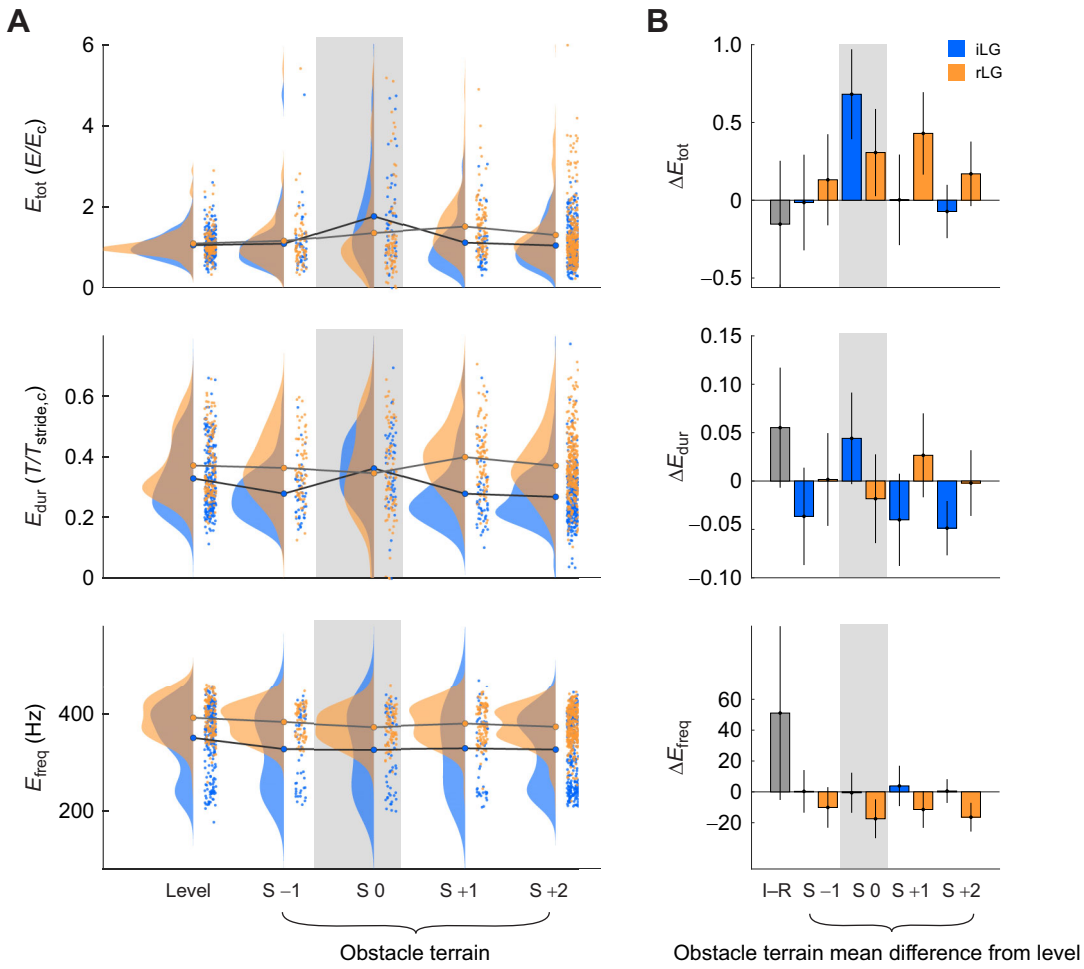

Fig. 4. Muscle activation across stride categories and surgical treatment. (A) Total integrated EMG per stride (E_{tot}, normalized to the level walking mean E_c), duration of EMG activity (E_{dur}, as a fraction of level stride duration $T_{stride,c}$), and EMG mean frequency (E_{freq}). Data distributions are shown for each stride category (level, S –1, S 0, S +1, S +2) for intact (blue) and reinnervated (orange) surgical conditions. (B) ANOVA *post hoc* pairwise mean differences (±95% CI) for fixed effect categories, between intact and reinnervated treatment cohorts (I–R, gray bars), and between obstacle stride categories compared with steady level walking (orange/blue bars), after accounting for the random effect of individual in the linear mixed-effect model.

late stance. rLG showed greater shortening during force development, with a more open work loop at high forces (Fig. 7). In obstacle terrain, LG work loop trajectories were similar to those in the level terrain condition in the non-perturbed strides (S −1, S +1, S +2) for both iLG and rLG (Fig. 4). In the obstacle contact strides (S 0), iLG exhibited an increase in both shortening and force, creating a more open work loop with a larger W_{net}. In comparison, F_{pk} of rLG was higher in obstacle strides, but net muscle shortening decreased slightly, resulting in a narrower work loop with little change in W_{net}.

Joint and CoM trajectory kinematics in intact and reinnervated birds

The trajectories of leg length and CoM height showed that intact birds adopted a more crouched posture in the obstacle strides (S 0), and returned to their typical posture in the unperturbed strides (S +2) (Fig. 8). In contrast, reinnervated birds adopted a more crouched posture across all stride categories, including level terrain, indicated by leg length as a fraction of total segment length (Fig. 8). Nonetheless, reinnervated birds showed a similar kinematic response to obstacles, with a decrease in effective leg length and CoM height in response to obstacle encounters (Fig. 8; Table S2). Knee and ankle angles were more flexed on average in the reinnervated birds (Fig. 8), with a significantly lower angle at contact across all strides (Tables S1 and S2). In obstacle strides, the ankle was more flexed at contact and showed net extension. In reinnervated birds, the ankle angle at the end of the S 0 stance was similar to the end-stance angle in level terrain, whereas in intact birds, the ankle remained more flexed than during level walking at the end of S 0 stance (Fig. 8; Table S2). Knee angles for reinnervated birds were more flexed at contact and showed reduced net flexion in S 0 compared with level strides (Fig. 8; Table S2). However, the difference in initial knee posture between S 0 and level strides was more pronounced in the intact birds. In reinnervated birds, reduced knee flexion with similar net ankle extension during the obstacle stride would tend to reduce the net change in length of the bi-articular LG muscle, which is consistent with the slower shortening velocity observed during the obstacle stance phase.

DISCUSSION

In the current study, we investigated how guinea fowl integrate *in vivo* muscle dynamics, sensorimotor control and kinematic movement strategies to maintain stable walking in response to obstacle perturbations. We hypothesized that LG proprioceptive

Journal of Experimental Biology (2023) 226, jeb245199. doi:10.1242/jeb.245199

Table 2. Linear mixed-effects ANOVA *F*-statistics, *post hoc* pairwise mean differences from ANOVA fixed effect

	F-statistics				Intact				Reinnervated			
Variable	Treatment	Stride ID	Interaction	Treatment cohort	S −1	S 0	S +1	S +2	S −1	S 0	S +1	S +2
E_{tot} (E/E_c)	0.5	19.3*	10.2*	−0.15±0.41	−0.01±0.31	0.68±0.29*	0.00±0.29	−0.07±0.17	0.13±0.29	0.31±0.28*	0.43±0.27*	0.17±0.21
E_{dur} ($T/T_{stride,c}$)	3.0	15.5*	11.3*	0.06±0.06	−0.04±0.05	0.04±0.05	−0.04±0.05	−0.05±0.03*	0.00±0.05	−0.02±0.05	0.03±0.04	0.00±0.03
E_{freq} (Hz)	3.2	0.3	5.7*	51±56	0±14	−1±13	4±13	1±8	−10±13	−17±13*	−11±12	−16±9*
E_{phase} (s)	1.7	4.2*	6.4*	−0.04±0.07	0.01±0.04	0.00±0.03	0.03±0.03	0.02±0.02*	0.00±0.03	0.06±0.03*	0.03±0.03	0.01±0.02
W_{net} (J kg^{-1})	0.1	101.1*	38.8*	−0.12±0.62	−0.52±0.72	3.64±0.68*	−0.34±0.68	−0.29±0.40	−0.10±0.68	0.72±0.66*	−0.07±0.62	0.06±0.49
F_{pk} (N)	0.1	17.7*	9.7*	0.01±0.10	−0.03±0.10	0.22±0.09*	0.01±0.09	0.02±0.05	0.09±0.09	0.43±0.09*	0.19±0.08*	0.12±0.07*
F_{dur} (s)	0.5	39.8*	2.2	0.02±0.06	−0.02±0.04	0.10±0.04*	−0.06±0.04*	−0.03±0.02*	−0.02±0.04	0.07±0.04*	−0.04±0.04*	−0.02±0.03
V_{pkF} (L_c s^{-1})	15.5*	13.9*	10.7*	−0.76±0.38*	0.31±0.42	−0.71±0.40*	0.15±0.40	0.09±0.24	0.20±0.40	0.27±0.38	0.20±0.36	0.12±0.28
$V_{mean,act}$	2.2	38*	24.6*	−0.26±0.35	0.16±0.21	−0.56±0.20*	0.28±0.20*	0.12±0.12*	0.17±0.20	0.21±0.20*	0.22±0.18*	0.15±0.14*
L_{pkF} (L/L_c)	0.2	87.3*	12.9*	−0.01±0.03	−0.01±0.02	0.10±0.02*	−0.01±0.02	−0.01±0.01	−0.03±0.02	0.09±0.02*	−0.07±0.02*	−0.02±0.01*
$L_{imp,T50}$ (L/L_c)	2.5	60.4*	22.2*	−0.02±0.02	−0.01±0.02	0.08±0.02*	0.00±0.02	−0.01±0.01	−0.02±0.02*	0.11±0.02*	−0.06±0.02*	−0.02±0.01*

F-statistics results for muscle dynamics variables with surgical treatment (Treatment), and stride ID as fixed categorical factors. Pairwise mean differences are shown between intact and reinnervated cohorts (Treatment cohort), between level and obstacle walking strides within each cohort. Means±s.d. Asterisks indicate statistical significance. See Materials and Methods for full details. E_{tot}, total integrated EMG per stride (normalized to the level mean E_c); E_{dur}, duration of EMG activity (as a fraction of level stride duration $T_{stride,c}$); E_{freq}, EMG mean frequency; E_{phase}, phase relationship between length and EMG as a fraction of stride cycle; W_{net}, net work output; F_{pk}, peak force; F_{dur}, force duration; V_{pkF}, muscle shortening velocity at peak force; $V_{mean,act}$, mean velocity during EMG activation; L_{pkF}, fractional muscle length at peak force; $L_{imp,T50}$, length at 50% force impulse; L/L_c, change in LG fractional length.

deficit would lead to decreased modulation of EMG activity in response to obstacle perturbations, with slower obstacle recovery compared with that for intact birds. We found that walking intact birds showed a one-stride recovery response, with a 68% increase in E_{tot} in the obstacle (S 0) stride compared with level strides, and no significant change in E_{tot} in S +1 or subsequent strides. Consistent with our hypothesis, birds with LG proprioceptive deficit showed a smaller, 31% increase in E_{tot} in S 0 compared with level terrain, and a 43% increase in E_{tot} on the S +1 recovery stride, indicating a multi-stride recovery. These findings are consistent with a deficit in reflex-mediated modulation of EMG activity in the immediate response to obstacle contact and indicate a slower recovery from obstacles in reinnervated compared with intact birds. Both iLG and rLG exhibited an increase in peak force in obstacle strides. However, net muscle work did not increase in rLG, in contrast to iLG. This indicates a shift in the mechanical role of the LG muscle in birds with a proprioceptive deficit to a more strut-like function with reduced work modulation. Interestingly, we also found guinea fowl with proprioceptive deficit adopt a more crouched posture during walking in both level and obstacle terrain.

Intact navigation of obstacles while walking

Intact birds walking over obstacle terrain recovered from perturbations within a single stride, using similar muscle mechanics to those previously found in running (Daley and Biewener, 2011). Intact LG showed increased EMG intensity (E_{tot}) in the obstacle encounter stride (S 0), yet returned to steady-state values in the first recovery stride (S +1), indicating a one-stride recovery response. In the obstacle stride, the increase in E_{tot} occurred with no change in phase or duration of activity but it did start after obstacle contact (Fig. 6), suggesting a reflex-mediated increase in amplitude without a change in timing. In running guinea fowl, iLG EMG activity increases in obstacle contact strides, but with an increase in duration of activity (Gordon et al., 2015, 2020). This likely reflects speed-related differences in feedback control, because there is more time within the stance period of walking for a reflex-mediated response. We note that the shape of the EMG trajectory tends to be idiosyncratic and unique to each individual, partly due to variation in motor patterns and partly due to varying EMG electrode geometry and placement. Therefore, we focused on comparing EMG summary values normalized as a fractional change from the steady-state level mean. The observed increases in iLG activity in obstacle strides occurred after obstacle contact, and after increases in length and force compared with the steady-state trajectory (Fig. 6). This suggests a reflex-mediated response rather than a feedforward increase in activation (Mortiz and Farley, 2004). The timing of increased EMG activity corresponds to a slight delay from the increase in force upon obstacle contact, consistent with positive force feedback, as has been found in cats (Donelan and Pearson, 2004; Donelan et al., 2009). In contrast, running guinea fowl show an anticipatory increase in EMG activation preceding obstacle-induced deviations in force and length, suggesting feedforward control mechanisms (Daley and Biewener, 2011; Gordon et al., 2020).

In addition to higher muscle activation in obstacle perturbed strides, LG force and work also increased significantly in S 0 compared with level terrain walking in the intact cohort. All other obstacle terrain strides were similar to those on level terrain, indicating a one-stride recovery response when walking over obstacles. The increased muscle work in intact birds occurred through increased force and higher shortening velocity in S 0, similar to running (Gordon et al., 2020). Kinematic patterns also reflected rapid obstacle recovery, with the intact birds adopting a

Journal of Experimental Biology (2023) 226, jeb245199. doi:10.1242/jeb.245199

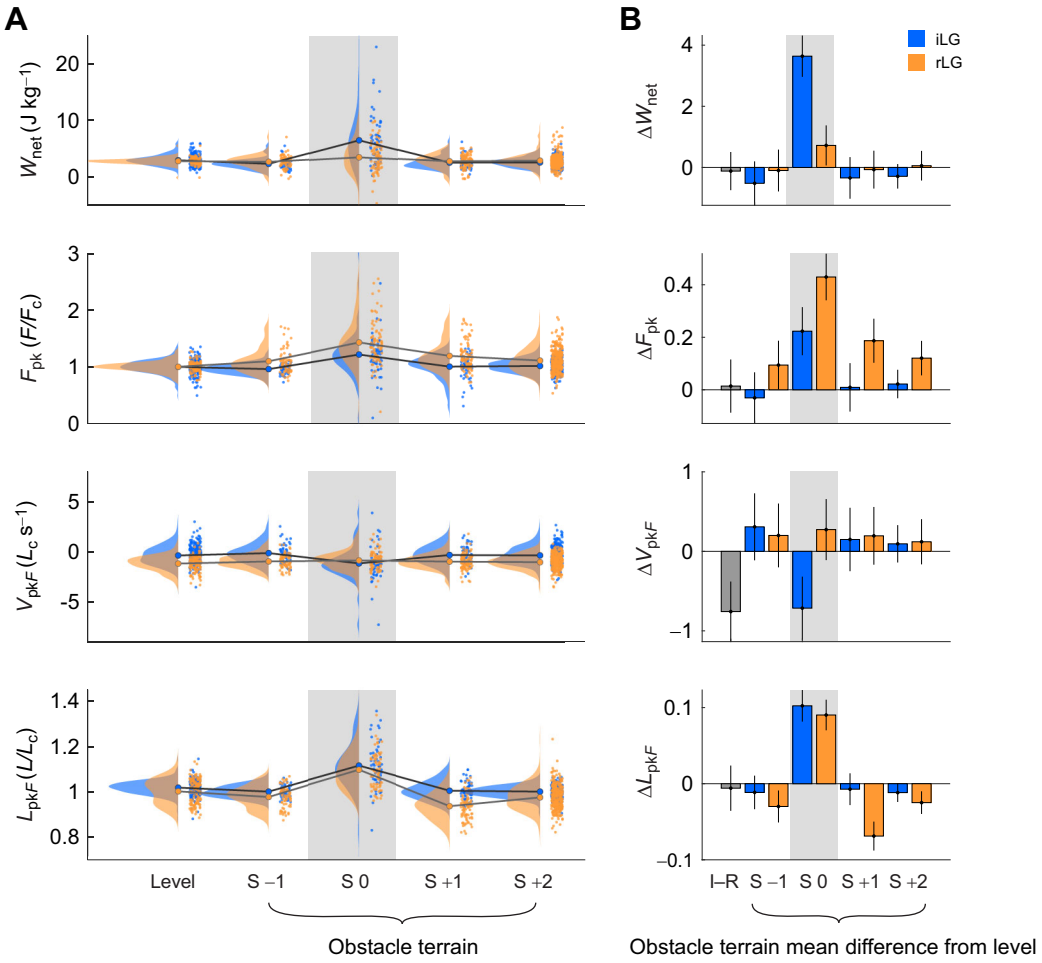

Fig. 5. Muscle mechanics across stride categories and surgical treatments. (A) Net work output (W_{net}), peak force (F_{pk}, normalized to peak force in level walking F_c), muscle shortening velocity at peak force (V_{pkF}) and fractional muscle length at peak force (L_{pkF}) normalized to fractional muscle length at peak force in level walking (L_c). Data distributions are shown for each stride category (level, S −1, S 0, S +1, S +2) for intact (blue) and reinnervated (orange) surgical conditions. (B) ANOVA *post hoc* pairwise mean differences (±95% CI) between intact and reinnervated treatment cohorts (I–R, gray bars), and between obstacle stride categories compared with steady level walking (orange/blue bars), after accounting for the random effect of individual in the linear mixed-effect model.

more crouched posture in the obstacle stride and recovering to normal posture before S +2.

Proprioceptive deficits and sensorimotor control

Guinea fowl with proprioceptive deficits in the LG exhibited a slower obstacle recovery compared with intact birds, with a pronounced change in obstacle negotiation strategy and muscle dynamics. rLG increased E_{tot} in S 0 by 31%, but with a significant delay in the phase of activation (E_{phase}; Table 2). Additionally, a larger, 43% increase in E_{tot} occurred in S +1, consistent with delayed reflexes. Analysis of the obstacle-perturbed trajectories compared with steady-state level showed that changes in EMG occur after deviations in length and force associated with obstacle contact, consistent with a reflex-mediated response; however, the changes in EMG were small and variable across individuals in rLG (Fig. 6). The observation that changes in muscle force and length occur before a change in EMG suggests that the changes in activity are likely to be feedback mediated and not feedforward mediated. The observed increase in force at the time of obstacle contact, without a change in EMG activity, likely occurs through a combination of factors including shifts in intrinsic mechanics and passive stiffness of connective tissues. Because of widespread interconnections of connective tissues, co-contraction of agonist or antagonist muscles in the distal leg could result in altered stiffness of the gastrocnemius in early stance, without a direct observable change in LG EMG activity. Nonetheless, we did find evidence for feedback-mediated muscle responses to obstacles in reinnervated birds, though smaller in amplitude and more variable compared with those for iLG. Hypothetically, if EMG activity increased before the time of foot contact, as observed during running (Gordon et al., 2020), this would suggest an anticipatory, feedforward increase in muscle activity. While it is feasible that reinnervated birds could anticipate obstacles and increase feedforward activation, we did not see evidence for this, because there is no change in EMG preceding altered loading in obstacle strides (Fig. 6). Reinnervated birds also exhibited larger deviations in LG length in response to obstacles in late stance, compared with intact birds, consistent with a deficit in reflex stiffness modulation. Feedforward increases in muscle activity, if they occurred, would be expected to help mitigate this deficit and minimize the perturbation induced by obstacle contact, but this was not observed.

In response to the obstacle perturbation, rLG peak muscle force increased, but with little change in shortening velocity and muscle work. By operating at low shortening velocity, the rLG exhibited a

Journal of Experimental Biology (2023) 226, jeb245199. doi:10.1242/jeb.245199

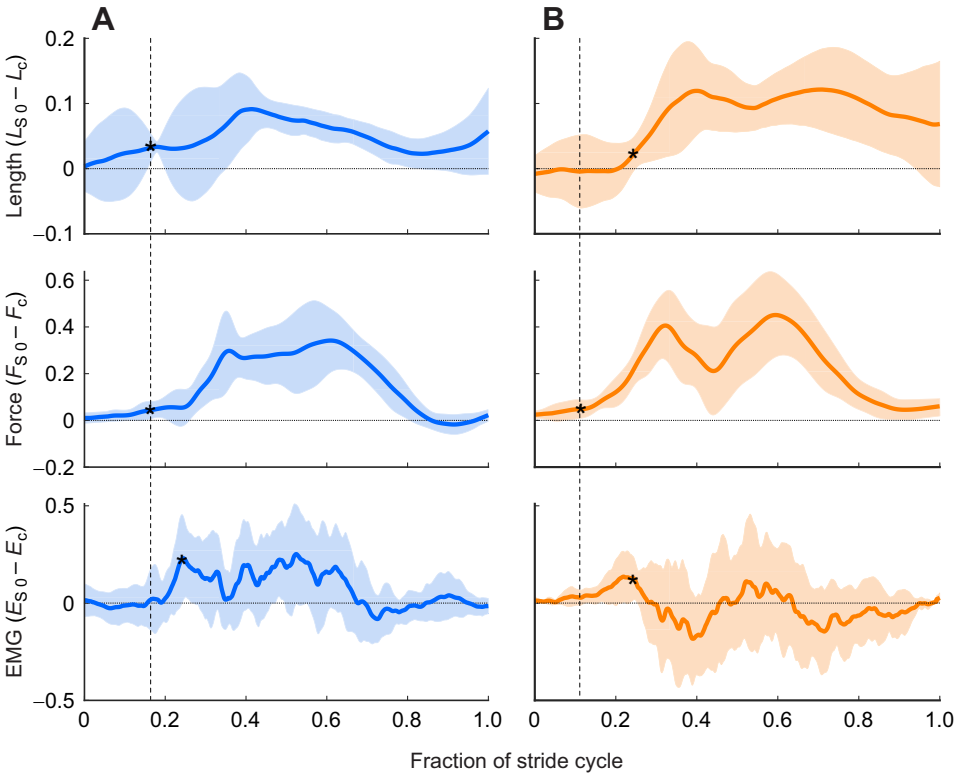

Fig. 6. Deviation from steady state in the obstacle stride cycle trajectories (S 0). Traces show the mean±95% CI (based on the grand mean ±95% CI across individuals) for muscle length, force and activation, calculated as the difference between obstacle and level strides, for (A) iLG and (B) rLG. The timing of obstacle contact is indicated by the vertical dashed line. The horizontal line at zero indicates no change from level walking. The stride cycle is from mid-swing to mid-swing. The asterisk indicates the first time point in the trajectory that significantly differs from the level mean. There is no evidence of an anticipatory increase in EMG preceding obstacle contact in either the intact or reinnervated cohort.

more strut-like function compared with the iLG. An increase in muscle–tendon force can enable energy transfer from more proximal muscles (Prilutsky and Zatsiorsky, 1994; Schwaner et al., 2018, 2021). Such energy transfer might allow proximal limb muscles to contribute work to compensate for the distal proprioceptive deficits.

In running birds, rLG exhibits work modulation with similar magnitude to that in intact birds, compensating for proprioceptive deficit through increased feedforward activation (Gordon et al., 2020). Our findings here suggest that birds compensate for proprioceptive deficit through different mechanisms between walking and running. In running, reinnervated birds compensated through a feedforward shift to an earlier onset of EMG activity, enabling an earlier rise of force to resist externally applied loads at the onset of foot contact. This allowed higher LG shortening velocity and muscle work during stance (Gordon et al., 2020). In walking, we did not see evidence of a feedforward increase in EMG to compensate for proprioceptive deficit (Fig. 6). The data for the current paper and that of Gordon and colleagues (2020) were taken from the same individuals. Consequently, the findings reveal flexibility in the mechanisms used to regulate the timing and intensity of muscle activation to achieve stability in different contexts. The importance of precise regulation of activation timing for regulation of muscle work output has also been demonstrated through controlled changes in activation during *in situ* cyclical work loop contractions (Sawicki et al., 2015).

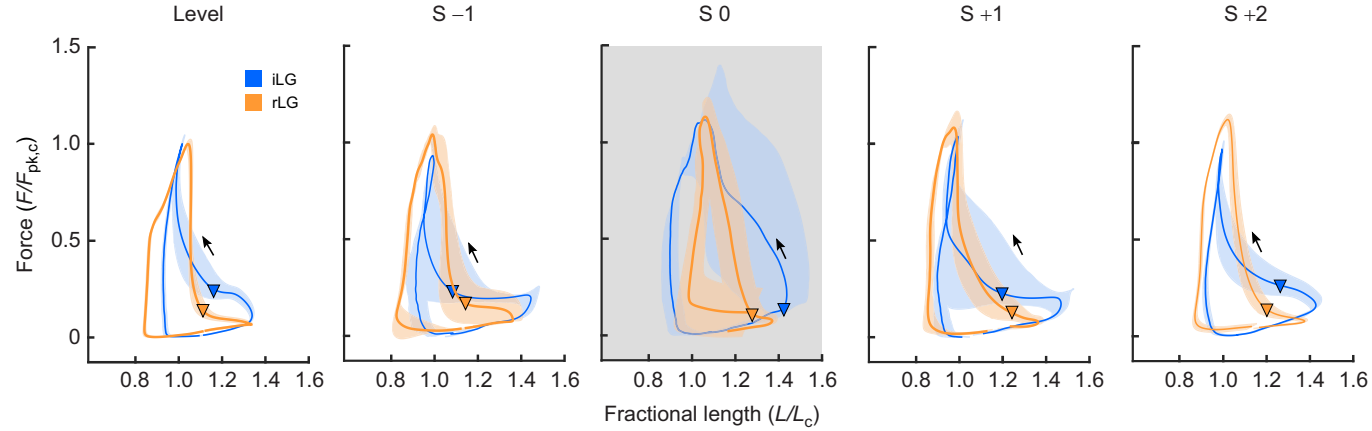

Fig. 7. Averaged LG work loop trajectories for each stride category for representative individuals from the intact (Ind 1) and reinnervated (Ind 13) cohorts. Traces show the mean±95% CI of force (normalized to peak force during level walking, $F/F_{pk,c}$) against fractional fascicle length (L/L_c). Arrows indicate the consistent counterclockwise direction of the work loops, indicating positive net work (W_{net}). Work loop trajectories are similar in level and non-perturbed (S −1, S +1, S +2) obstacle terrain strides. In obstacle strides (S 0), iLG exhibits an increase in both shortening and force, creating a more open loop with larger W_{net}. In rLG, peak force increases but shortening decreases slightly, resulting in a narrower work loop with little change in W_{net}.

Journal of Experimental Biology (2023) 226, jeb245199. doi:10.1242/jeb.245199

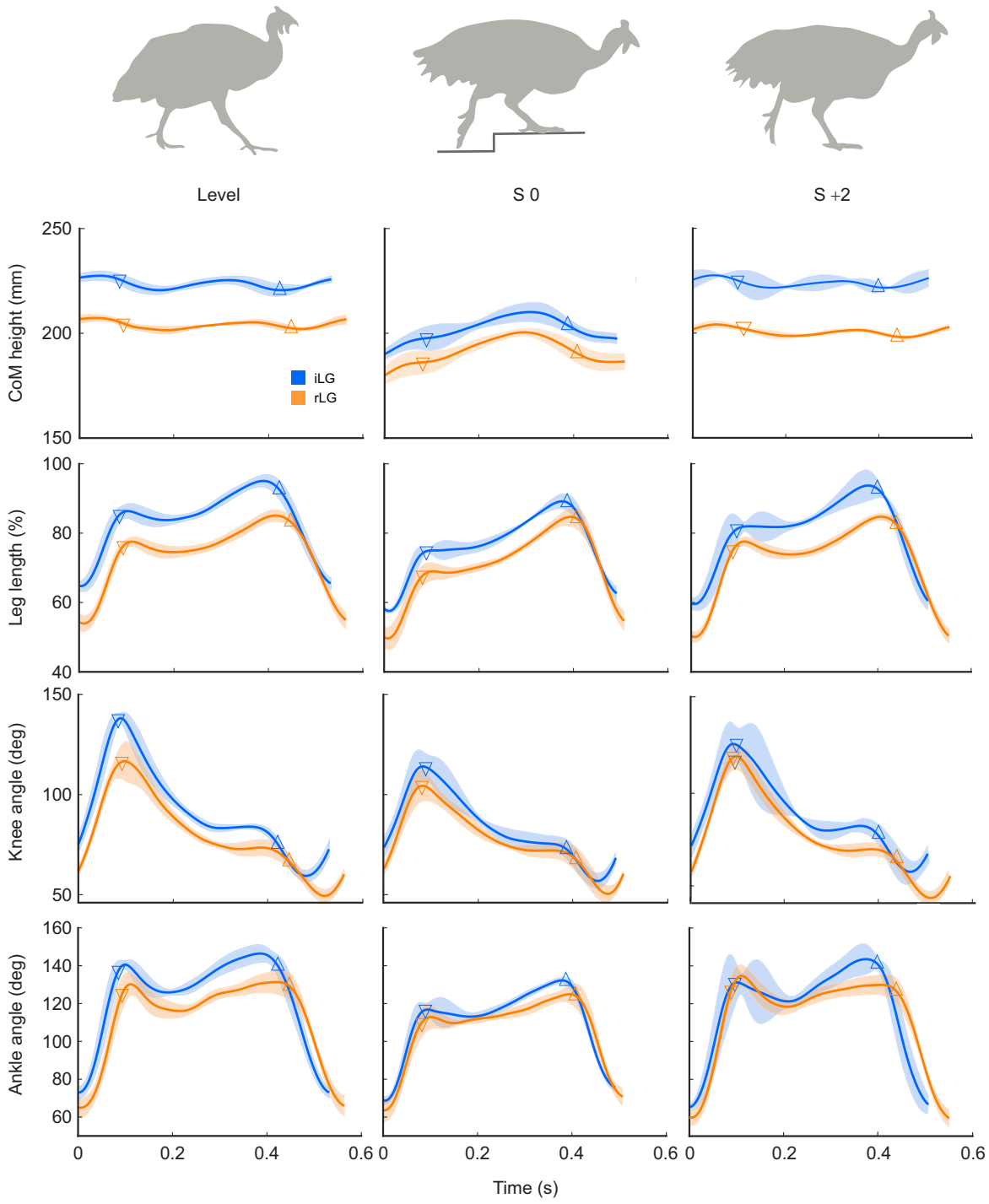

Fig. 8. Group mean kinematic trajectories during level strides, obstacle strides (S 0) and second recovery strides (S +2) in obstacle terrain for the intact and reinnervated cohorts. Traces show the mean±95% CI for center of mass (CoM) height, leg length, knee angle and ankle angle. CoM height is the vertical distance between the CoM and foot height (measured at mid stance). Leg length is shown as a percentage of total available leg length (sum of all segment lengths). Downward pointing triangles indicate time of foot on (T_{on}) and upward pointing triangles indicate time of foot off (T_{off}). Intact birds adopt a more crouched posture in the obstacle strides only and return to their typical posture in the unperturbed strides (S +2). Reinnervated birds adopt a more crouched posture across all stride categories, including level walking, but also show a more substantial decrease in CoM height and effective leg length in obstacle strides. Altered leg posture and CoM height result from increased flexion in the knee and ankle at T_{on}.

Proprioceptive deficit compensation through postural changes

Leg length change plays an important role during perturbation responses. For example, when guinea fowl encounter an unexpected drop in terrain, they maintain similar CoM trajectories to those for level running through increased leg extension, although the perturbation causes a large drop of the bird's foot (Daley and Biewener, 2006; Blum et al., 2011; Müller et al., 2016). Humans use similar strategies when navigating surfaces of different stiffness during running (Ferris et al., 1998). Walking birds adopt a slightly

more crouched posture when exposed to treadmill belt speed perturbations (Schwaner et al., 2022). Here, we observed that guinea fowl also compensated for proprioceptive deficits in the LG muscle by adopting a more crouched posture across all walking conditions (level and obstacle terrain). The crouched posture occurred through increased ankle and knee flexion, resulting in shorter effective leg length and lower CoM height (Fig. 8). Adopting a more crouched posture likely increases passive tension in the muscle–tendon system, increasing effective muscle stiffness. However, crouched posture also decreases effective mechanical advantage, leading to lower joint and leg stiffness relative to muscle stiffness (McMahon et al., 1987; Biewener, 1989; Gatesy and Biewener, 1991; Reinboldt et al., 2009; Steele et al., 2012). Crouched posture and higher leg compliance during running are linked to increased stability and robustness to changes in terrain height (Daley and Usherwood, 2010; Blum et al., 2011; Müller et al., 2016). However, crouched posture requires higher muscle forces to resist a given ground reaction force and can be associated with increased metabolic cost (McMahon et al., 1987). Like guinea fowl, humans also show concurrent increases in crouched posture, muscle activation and force, following nerve and muscle impairments (Reinboldt et al., 2009; Hoang and Reinbolt, 2012; Spomer et al., 2022).

Our results highlight locomotor resilience as reinnervated birds compensate for proprioceptive loss through multiple mechanisms to maintain stable locomotion. Postural adaptation, as observed in our reinnervated cohort, has stability benefits (e.g. Blum et al., 2011) but also co-occurs with changes in muscle dynamics. Reinnervated LG muscles adopted a more strut-like isometric function, with an increase in force but a decrease in work modulation. These changes in LG muscle dynamics may help mitigate postural costs, as greater muscle forces are countered with reduced muscle work and more strut-like function. High force in a bi-articular LG muscle likely also enables greater energy transfer from more proximal limb muscles through the linkage between the knee and ankle. The observed change in obstacle negotiation strategy in reinnervated walking suggests that neuromechanical versatility may be higher in walking than in running. Walking is a submaximal behavior that might provide a broader array of neuromechanical solutions to maintain stable locomotion in response to external (e.g. obstacles) and internal (e.g. loss of proprioception) perturbations.

Conclusion

In this study, we investigated how walking guinea fowl navigate obstacle terrain, and how they compensate for proprioceptive deficit to maintain stable locomotion. Compared with intact birds, guinea fowl with reinnervated LG exhibited a delayed and prolonged recovery response and adopted a more crouched posture during walking. We found that reinnervated birds compensate for proprioceptive loss through intrinsic muscle mechanics, shifting toward more strut-like function. This suggests a potential role for more proximal muscles contributing to the stability control of walking with a proprioceptive deficit, through proximal-to-distal muscle work transfer via the LG muscle–tendon unit. Future research combining *in vivo* measurement from multiple muscles with predictive musculoskeletal modeling could provide further insights for how muscles are coordinated to achieve robust locomotion while navigating complex terrain at both slow and fast speeds.

Acknowledgements

The authors would like to acknowledge Jennifer A. Carr and Natalie C. Holt for their assistance during experiments.

Competing interests

The authors declare no competing or financial interests.

Author contributions

Conceptualization: J.C.G., A.A.B., M.A.D.; Methodology: J.C.G., A.A.B.; Software: M.J.S.; Validation: J.C.G., A.A.B., M.A.D.; Formal analysis: M.J.S., M.A.D.; Investigation: M.J.S., J.C.G., A.A.B., M.A.D.; Resources: M.A.D., A.A.B.; Data curation: M.J.S., J.C.G.; Writing - original draft: M.J.S., M.A.D.; Writing - review & editing: M.J.S., J.C.G., A.A.B., M.A.D.; Visualization: M.J.S., M.A.D.; Supervision: M.A.D.; Project administration: M.A.D.; Funding acquisition: J.C.G., A.A.B., M.A.D.

Funding

This work was supported by the National Institutes of Health (NIAMS 5R01AR055648 to A.A.B), Biotechnology and Biological Sciences Research Council (Doctoral training studentship to J.C.G, M.A.D.), and National Science Foundation (2016049 to M.A.D).

Data availability

The kinematics data for walking and running, and muscle dynamics of walking intact and reinnervated birds reported in this article are available from the Dryad digital repository (Schwaner et al., 2023): https://doi.org/10.5061/dryad.t1g1jwt5q.

ECR Spotlight

This article has an associated ECR Spotlight interview with Janneke Schwaner.

References

Abelew, T. A., Miller, M. D., Cope, T. C. and Nichols, T. R. (2000). Local loss of proprioception results in disruption of interjoint coordination during locomotion in the cat. *J. Neurophysiol.* **84**, 2709-2714. doi:10.1152/jn.2000.84.5.2709

Bauman, J. M. and Chang, Y. H. (2013). Rules to limp by: joint compensation conserves limb function after peripheral nerve injury. *Biol. Lett.* **9**, 20130484. doi:10.1098/rsbl.2013.0484

Biewener, A. A. (1989). Scaling body support in mammals: limb posture and muscle mechanics. *Science. Wash* **245**, 45-48. doi:10.1126/science.2740914

Birn-Jeffery, A. V., Hubicki, C. M. and Blum, Y. (2014). Don't break a leg: running birds from quail to ostrich prioritize leg safety and economy on uneven terrain. *J. Exp. Biol.* **217**, 3786-3797. doi:10.1242/jeb.102640

Blum, Y., Birn-Jeffery, A., Daley, M. A. and Seyfarth, A. (2011). Does a crouched leg posture enhance running stability and robustness? *J. Theor. Biol.* **281**, 97-106. doi:10.1016/j.jtbi.2011.04.029

Brown, I. E. and Loeb, G. E. (2000). A reductionist approach to creating and using neuromechanical models. In *Biomechanics and Neural Control of Posture and Movement* (, ed. J. M. Winters and P. E. Crago), pp. 148-163. New York: Springer-Verlag.

Capaday, C. and Stein, R. B. (1987). Difference in the amplitude of the human soleus H reflex during walking and running. *J. Physiol.* **392**, 513-522. doi:10.1113/jphysiol.1987.sp016794

Cavagna, G. A. and Kaneko, M. (1977). Mechanical work and efficiency in level walking and running. *J. Physiol.* **268**, 467-481. doi:10.1113/jphysiol.1977.sp011866

Chang, Y. H., Auyang, A. G., Scholz, J. P. and Nichols, T. R. (2009). Whole limb kinematics are preferentially conserved over individual joint kinematics after peripheral nerve injury. *J. Exp. Biol.* **212**, 3511-3521. doi:10.1242/jeb.033886

Chang, Y. H., Housley, S. N., Hart, K. S., Nardelli, P., Nichols, R. T., Maas, H. and Cope, T. C. (2018). Progressive adaptation of whole-limb kinematics after peripheral nerve injury. *Biol. Open* **7**, bio028852. doi:10.1242/bio.028852

Daley, M. A. and Biewener, A. A. (2003). Muscle force-length dynamics during level versus incline locomotion: a comparison of *in vivo* performance of two guinea fowl ankle extensors. *J. Exp. Biol.* **206**, 2941-2958. doi:10.1242/jeb.00503

Daley, M. A. and Biewener, A. A. (2006). Running over rough terrain reveals limb control for intrinsic stability. *Proc. Natl. Acad. Sci. USA* **103**, 15681-15686. doi:10.1073/pnas.0601473103

Daley, M. A. and Biewener, A. A. (2011). Leg muscles that mediate stability: mechanics and control of two distal extensor muscles during obstacle negotiation in the guinea fowl. *Philos. Trans. R. Soc. Lond. B Biol. Sci.* **366**, 2693-2707. doi:10.1098/rstb.2010.0338

Daley, M. A. (2018). Understanding the agility of running birds: sensorimotor and mechanical factors in avian bipedal locomotion. *Integr. Comp. Biol.* **58**, 884-893.

Daley, M. A., Felix, G. and Biewener, A. A. (2007). Running stability is enhanced by a proximo-distal gradient in joint neuromechanical control. *J. Exp. Biol.* **210**, 383-394. doi:10.1242/jeb.02668

Daley, M. A. and Usherwood, J. R. (2010). Two explanations for the compliant running paradox: reduced work of bouncing viscera and increased stability in uneven terrain. *Biol. Lett.* **6**, 418-421. doi:10.1098/rsbl.2010.0175

Daley, M. A., Voloshina, A. and Biewener, A. A. (2009). The role of intrinsic muscle mechanics in the neuromuscular control of stable running in guinea fowl. *J. Physiol.* **587**, 2693-2707. doi:10.1113/jphysiol.2009.171017

Dickinson, M. H., Farley, C. T., Full, R. J., Koehl, M. A. R., Kram, R. and Lehman, S. (2000). How animals move: an integrative view. *Science* **288**, 100-106. doi:10.1126/science.288.5463.100
Dietz, V., Schmidtbleicher, D. and Noth, J. (1979). Neuronal mechanisms of human locomotion. *J. Neurophysiol.* **42**, 1212-1222. doi:10.1152/jn.1979.42.5.1212
Donelan, J. M. and Pearson, K. G. (2004). Contribution of force feedback to ankle extensor activity in decerebrate walking cats. *J. Neuro. Physiol.* **92**, 2093-2104.
Donelan, J. M., McVea, D. A. and Pearson, K. G. (2009). Force regulation of ankle extensor muscle activity in freely walking cats. *J. Neurophysiol.* **101**, 360-371. doi:10.1152/jn.90918.2008
Edamura, M., Yang, J. F. and Stein, R. B. (1991). Factors that determine the magnitude and time course of human H-reflexes in locomotion. *J. Neurosci.* **11**, 420-427. doi:10.1523/JNEUROSCI.11-02-00420.1991
Farley, C. T., Glasheen, J. and McMahon, T. A. (1993). Running springs: speed and animal size. *J. Exp. Biol.* **185**, 71-86. doi:10.1242/jeb.185.1.71
Farley, C. T. and Farris, D. P. (1998). Biomechanics of walking and running: center of mass movements to muscle action. *Exerc. Sport Sci. Rev.* **28**, 253-285.
Ferris, D. P., Louie, M. and Farley, C. T. (1998). Running in the real world: adjusting leg stiffness for different surfaces. *Proc. R. Soc. B* **265**, 989-994. doi:10.1098/rspb.1998.0388
Frigon, A. and Rossignol, S. (2006). Experiments and models of sensorimotor interactions during locomotion. *Biol. Cybern.* **95**, 607-627. doi:10.1007/s00422-006-0129-x
Gatesy, S. M. (1999). Guineafowl hind limb function. I: Cineradiographic analysis and speed effects. *J. Morphol.* **240**, 115-125. doi:10.1002/(SICI)1097-4687(199905)240:2<115::AID-JMOR3>3.0.CO;2-Y
Gatesy, S. M. and Biewener, A. A. (1991). Bipedal locomotion: effect of speed, size and limb posture in birds and humans. *J. Zool.* **224**, 137-147. doi:10.1111/j.1469-7998.1991.tb04794.x
Geyer, H., Seyfarth, A. and Blickhan, R. (2006). Compliant leg behaviour explains basic dynamics of walking and running. *Proc. R. Soc. Lond. B Biol. Sci.* **271**, 2861-2867.
Gordon, J. C., Rankin, J. W. and Daley, M. A. (2015). How do treadmill speed and terrain visibility influence neuromuscular control of guinea fowl locomotion? *J. Exp. Biol.* **218**, 3010-3022. doi:https://doi.org/10.1242/jeb.104646
Gordon, J. C., Holt, N. C., Biewener, A. A. and Daley, M. A. (2020). Tuning of feedforward control enables stable muscle force-length dynamics after loss of autogenic proprioceptive feedback. *Elife* **9**, e53908. doi:10.7554/eLife.53908
Hoang, H. X. and Reinbolt, J. A. (2012). Crouched posture maximizes ground reaction forces generated by muscles. *Gait Posture* **36**, 405-408. doi:10.1016/j.gaitpost.2012.03.020
Jindrich, D. L. and Full, R. J. (2002). Dynamic stabilization of rapid hexapedal locomotion. *J. Exp. Biol.* **205**, 2803-2823. doi:10.1242/jeb.205.18.2803
Maas, H., Prilutsky, B. I., Nichols, T. R. and Gregor, R. J. (2007). The effect of self-reinnervation of cat medial and lateral gastrocnemius muscles on hindlimb kinematics in slope walking. *Exp. Brain Res.* **181**, 377-393. doi:10.1007/s00221-007-0938-8
Mathis, A., Mamidanna, P., Cury, K. M., Abe, T., Murthy, V. N., Mathis, M. W. and Bethge, M. (2018). DeepLabCut: markerless pose estimation of user-defined body parts with deep learning. *Nat. Neurosci.* **21**, 1281-1289. doi:10.1038/s41593-018-0209-y
McGeer, T. (1990a). Passive bipedal running. *Proc. R. Soc. Lond. B Biol. Sci. B* **240**, 107-134. doi:10.1098/rspb.1990.0030
McGeer, T. (1990b). Passive dynamic walking. *Int. J. Rob. Res.* **9**, 62-82. doi:10.1177/027836499000900206
McMahon, T. A. and Cheng, G. C. (1990). The mechanics of running: how does stiffness couple with speed? *J. Biomech.* **23**, 65-78. doi:10.1016/0021-9290(90)90042-2
McMahon, T. A., Valiant, G. and Frederic, E. C. (1987). Croucho running. *J. Appl. Physiol.* **18**, 367-370.
More, H. L. and Donelan, J. M. (2018). Scaling of sensorimotor delays in terrestrial mammals. *Proc. Biol. Sci.* **285**, 20180613.
Mortiz, C. T. and Farley, C. T. (2004). Passive dynamics change leg mechanics for an unexpected surface during human hopping. *J. Appl. Physiol.* **97**, 1313-1322. doi:10.1152/japplphysiol.00393.2004
Müller, R., Birn-Jeffery, A. V. and Blum, Y. (2016). Human and avian running on uneven ground: a model-based comparison. *J. R Soc. Interface* **13**, 20160529. doi:10.1098/rsif.2016.0529
Nath, T., Mathis, A., Chen, A. C., Patel, A., Bethge, M. and Mathis, M. W. (2019). Using DeepLabCut for 3D markerless pose estimation across species and behaviors. *Nat. Protoc.* **14**, 2152-2176. doi:10.1038/s41596-019-0176-0
Nishikawa, K. C., Biewener, A. A., Aerts, P., Ahn, A. N., Chile, H. J., Daley, M. A., Daniel, T. L., Full, R. J., Hale, M. E., Hedrick, T. L. et al. (2007). Neuromechanics: an integrative approach for understanding motor control. *Integr. Comp. Biol.* **47**, 16-54. doi:10.1093/icb/icm024
Pearson, K. G. (2000). Neural adaptation in the generation of rhythmic behavior. *Annu. Rev. Physiol.* **62**, 723-753. doi:10.1146/annurev.physiol.62.1.723
Prilutsky, B. I. Zatsiorsky, V. M. (1994). Tendon action of two-joint muscles: transfer of mechanical energy between joints during jumping, landing, and running. *J. Biomech.* **27**, 25-34. doi:10.1016/0021-9290(94)90029-9
Prochazka, A. and Ellaway, P. (2012). Sensory systems in the control of movement. *Compr. Physiol.* **2**, 2615-2627. doi:10.1002/cphy.c100086
Reinboldt, J. A., Seth, A., Hicks, J. L. and Delp, S. L. (2009). Mechanical advantage of crouch gait. XII International Symposium on Computzer Simulation in Biomechanics, July 2009, Cape Town, South Africa.
Rubenson, J. and Marsh, R. L. (2003). Mechanical efficiency of limb swing during walking and running in guinea fowl (*Numida meleagris*). *J. Appl. Physiol.* **106**, 1618-1630. doi:10.1152/japplphysiol.91115.2008
Sawicki, G. S., Robertson, B. D., Azizi, E. and Roberts, T. J. (2015). Timing matters: tuning the mechanics of a muscle-tendon unit by adjusting stimulation phase during cyclic contractions. *J. Exp. Biol.* **218**, 3150-3159.
Schwaner, M. J., Lin, D. C. and McGowan, C. P. (2018). Jumping mechanics of desert kangaroo rats. *J. Exp. Biol.* **221**, jeb186700. doi:10.1242/jeb.186700
Schwaner, M. J., Lin, D. C. and McGowan, C. P. (2021). Plantar flexor muscles of kangaroo rats (*Dipodomys deserti*) shorten at a velocity to produce optimal power during jumping. *J. Exp. Biol.* **224**, jeb242630. doi:10.1242/jeb.242630
Schwaner, M. J., Nishikawa, K. C. and Daley, M. A. (2022). Kinematic trajectories in response to speed perturbations in walking suggest modular task-level control of leg angle and length. *Int. Comp. Biol.* **2022**, icac057.
Schwaner, M. J., Gordon, J. C., Biewener, A. A. and Daley, M. A. (2023). Data from: Muscle force-length dynamics during walking over obstacles indicates delayed recovery and a shift towards more strut-like function in birds with proprioceptive deficit. Dryad, Dataset. https://doi.org/10.5061/dryad.t1g1jwt5q
Spomer, A. M., Yan, R. Z., Schwartz, M. H. and Steele, K. M. (2022). Synergies are minimally affected during emulation of cerebral palsy gait patterns. *J. Biomech.* **133**, 110953. doi:10.1016/j.jbiomech.2022.110953
Steele, K. M., DeMers, M. S., Schwartz, M. H. and Delp, S. L. (2012). Compressive tibiofemoral force during crouch gait. *Gait Posture* **35**, 556-560. doi:10.1016/j.gaitpost.2011.11.023
Stein, R. B. and Capaday, C. (1988). The modulation of human reflexes during functional motor tasks. *Trends Neurosci.* **11**, 328-332. doi:10.1016/0166-2236(88)90097-5
Von Tscharner, V. (2000). Intensity analysis in time-frequency space of surface myoelectric signals by wavelets of specified resolution. *J. Electromyogr. Kinesiol.* **10**, 433-445. doi:10.1016/S1050-6411(00)00030-4
Wakeling, J. M., Kaya, M., Temple, G. K., Johnston, I. A. and Herzog, W. (2002). Determining patterns of motor recruitment during locomotion. *J. Exp. Biol.* **205**, 359-369. doi:10.1242/jeb.205.3.359
Wilmink, R. J. H. and Nichols, T. R. (2003). Distribution of heterogenic reflexes among the quadriceps and triceps surae muscle of the cat hindlimb. *J of Neurophysiology* **90**, 2310-2324. doi:10.1152/jn.00833.2002

Table S1. Linear mixed effect model ANOVA F-statistics results with stride ID and surgical treatment as fixed categorical factors kinematic variables. Values accompanied by an asterisk indicate statistical significance. See methods for full details.

	F-statistic		
Variable	***treatment***	***stride ID:***	***interaction***
StridePeriod (ms)	0.57	1.32	**2.90***
StancePeriod (ms)	0.42	1.17	**3.74***
CoM H $_{Ton}$ (mm)	**9.05***	**27.32***	**5.73***
Δ COM H (mm)	0.15	1.76	1.28
LA$_{Ton}$ (°)	2.43	1.28	0.65
LA$_{net}$ (°)	1.92	0.84	1.67
LL $_{Ton}$ (mm)	**15.13***	**35.39***	**8.00***
LL $_{net}$ (mm)	0.25	1.36	**4.38***
Ankle $_{Ton}$ (°)	**10.71***	**20.12***	**3.15***
Ankle$_{net}$ (°)	0.00	1.44	2.21
Ankle $_{max}$ (°)	2.86	**4.40***	**3.63***
Knee $_{Ton}$ (°)	**12.85***	**23.61***	**11.01***
Knee$_{net}$ (°)	4.14	**6.11***	4.86*
Knee$_{max}$ (°)	3.23	**5.64***	**4.35***
TMP $_{Ton}$ (°)	0.04	**5.60***	**2.93***
TMP $_{net}$ (°)	3.52	1.48	0.59
TMP $_{max}$ (°)	1.03	0.38	0.55
Hip $_{Ton}$ (°)	1.87	**10.88***	**5.13***
Hip$_{net}$ (°)	2.43	**5.59***	**3.87***

Table S2. Linear mixed-effects model ANOVA pairwise difference between obstacle strides and level walking for kinematic dynamics variables. Bold values with accompanying asterisks indicate statistical significance.

		Intact				Reinnervated			
Variable	**Treatment cohort**	**S -1**	**S 0**	**Str +1**	**S +2**	**S -1**	**S 0**	**Str +1**	**S +2**
StridePeriod	25.1±65.0	-20.8±45.7	**-49.9±40.9***	**-50.4±42.9***	-14.8±34.3	3.4±27.7	**-44.7±27.5***	**-84.3±27.7***	-10.6±24.2
StancePeriod	18.5±56.3	-31.1±43.9	-20.5±39.3	**-46.0±41.3***	-10.2±33.0	-2.3±26.6	-15.8±26.4	**-80.5±26.6***	-1.2±23.2
CoM H $_{Ton}$	**-29.2±19.1***	-8.1±9.0	**-49.6±8.1***	-1.7±8.5	**-7.4±6.8***	0.4±5.5	**-45.2±5.4***	**12.8±5.5***	-1.6±4.8
COM$_{net}$	0.9±4.7	2.3±11.4	8.7±10.2	**-15.1±10.7***	0.0±8.6	3.7±6.9	6.0±6.8	**-22.4±6.9***	-0.9±6.0
LA $_{Ton}$	-4.5±5.7	-2.1±3.2	-0.4±2.9	0.5±3.0	-1.8±2.4	-0.5±2.0	0.1±1.9	1.5±2.0	-0.5±1.7
LA$_{net}$	4.1±5.8	1.1±4.7	4.2±4.2	1.5±4.4	2.9±3.5	-0.7±2.8	**6.1±2.8***	0.7±2.8	1.3±2.5
LL $_{Ton}$	**-9.2±4.6***	**-4.8±3.1***	**-17.8±2.8***	**-7.2±2.9***	**-4.5±2.3***	**-2.9±1.9***	**-15.2±1.9***	-1.2±1.9	**-2.1±1.6**
LL$_{net}$	-1.1±4.3	2.6±5.0	**5.5±4.5***	3.9±4.7	1.7±3.8	**3.7±3.1***	**9.9±3.0***	0.8±3.1	1.2±2.7
Ankle $_{Ton}$	**-13.7±8.2***	-6.5±7.9	**-34.5±7.0***	-5.8±7.4	-5.4±5.9	-3.4±4.8	**-28.8±4.7***	3.5±4.8	-1.1±4.2
Ankle$_{net}$	0.3±12.0	4.2±10.4	**12.2±9.3**	3.0±9.8	3.6±7.8	1.4±6.3	**11.9±6.3***	-6.1±6.3	-2.1±5.5
Ankle$_{max}$	6.9±8.0	3.9±6.4	**9.2±5.7***	2.8±6.0	3.2±4.8	2.5±3.9	3.3±3.8	**-4.5±3.9***	0.2±3.4
Knee $_{Ton}$	**-24.2±13.2***	**-11.9±8.0***	**-30.8±7.2***	**-9.4±7.5***	**-10.8±6.0***	0.6±4.9	**-16.6±4.8***	**5.3±4.9***	1.5±4.2
Knee$_{net}$	**12.0±11.6***	**13.1±8.8***	**17.4±7.9***	7.9±8.3	**7.6±6.6***	4.6±5.4	**14.7±5.3***	-3.2±5.4	-1.2±4.7
Knee$_{max}$	10.1±11.1	**9.5±7.2***	**16.0±6.4***	5.2±6.7	**6.3±5.4***	2.9±4.4	**14.9±4.3***	-3.0±4.4	0.0±3.8
TMP$_{Ton}$	0.7±7.0	4.5±5.1	**11.9±4.5***	3.6±4.8	1.9±3.8	0.7±3.1	**11.1±3.0***	-1.7±3.1	0.0±2.7
TMP$_{net}$	-9.3±9.8	-5.0±11.6	-10.4±10.3	-3.2±10.9	0.4±8.7	0.4±7.0	**-8.2±7.0***	-0.2±7.0	0.6±6.1
TMP$_{max}$	-5.1±9.8	-0.7±9.0	-1.1±8.0	1.0±8.4	0.9±6.7	-1.0±5.4	1.8±5.4	1.2±5.4	-0.3±4.7
Hip $_{Ton}$	-6.7±9.6	**-8.4±5.0***	**-14.2±4.4***	-4.3±4.7	**-7.6±3.7***	-2.6±3.0	**-12.5±3.0***	-3.1±3.0	-2.0±2.6
Hip$_{net}$	5.4±6.8	**8.2±6.4***	**10.3±5.7***	5.3±6.0	**6.5±4.8***	0.8±3.9	**7.4±3.8***	3.1±3.9	0.3±3.4